Journal of Chromatography A, 1266 (2012) 24–33

Contents lists available at SciVerse ScienceDirect

Journal of Chromatography A

journal homepage: www.elsevier.com/locate/chroma

Experimental and theoretical studies on the enantioselectivity of molecularly imprinted polymers prepared with a chiral functional monomer

Juan J. Torres[a], Natalia Gsponer[a], Cristina L. Ramírez[b], D. Mariano A. Vera[b], Hernán A. Montejano[a], Carlos A. Chesta[a,*]

[a] Departamento de Química, Facultad de Ciencias Exactas, Físico-Químicas y Naturales, Universidad Nacional de Río Cuarto, 5800 Río Cuarto, Argentina
[b] Departamento de Química, Facultad de Ciencias Exactas y Naturales, Universidad Nacional de Mar del Plata, Funes 3350, 7600 Mar del Plata, Argentina

ARTICLE INFO

Article history:
Received 23 May 2012
Received in revised form 19 August 2012
Accepted 14 September 2012
Available online 25 September 2012

Keywords:
Molecularly imprinted polymers
Adsorption isotherms
HPLC
Binding site's distribution
Racemic resolution

ABSTRACT

A comprehensive study on the enantioseparation of racemic bis[1-phenylethyl]amine (PEA) on a series of molecularly imprinted polymers (MIPs) prepared using the chiral functional monomer (S)-2-(2-methyl-acryloylamino)-3-phenyl propionic acid (MAPP) is reported. MIP-R, MIP-S and MIP-RS, were synthesized separately by imprinting the pure enantiomers (R-, S-PEA) and racemic PEA, respectively, MAPP, EDGMA as crosslinker and chloroform as the porogen. It was found that all MIPs prepared were able to resolve the PEA racemate. Residence times (t_r) and enantioselectivity factors (α) were estimated from typical elution chromatography experiments. Frontal chromatography experiments were conducted to acquire the adsorption isotherms for both enantiomers on the different MIPs (and on the non-imprinted polymer, NIP). The adsorption isotherms were analyzed using the affinity spectrum (AS) and the expectation-maximization (EM) methods. The study also involved the theoretical evaluation of the MAPP/enantiomers interactions in the pre-polymer mixture. The EM method predicts mono- and bimodal distribution of affinity binding sites depending upon the polymer analyzed. Apparently, the enantioseparation process depends on relatively small differences in the stabilization of the diasteroisomeric ion-pairs PEA/MAPP complexes on the surface of the polymers.

1. Introduction

Molecular imprinting is a simple technique to fabricate polymeric matrix with molecular-specific recognition sites for practically any compound of interest using the same compound as template [1]. This technique has gained substantial attention as a means for achieving functional materials for applications including chromatographic separations [2–4], molecular sensing [5], drug delivery [6], enzyme catalysis mimicking [7], etc.

Probably, one of the most appealing applications of MIPs is their use as HPLC stationary phase for racemic resolution [8]. The enantioseparation of small organic molecules is one of the most important challenges in separation science and of enormous importance to pharmaceuticals and many other fields of chemistry [9]. Several examples of MIPs prepared to this end have been reported [8,10–12]. It is worth to note that the conventional approach for the synthesis of chiral MIPs requires pure enantiomers as templates. Generally, enantiomers are expensive and considerable amounts (~100 mg) are required for the production of a simple (analytical) column. Evidently, prohibitive quantities would be needed to prepare MIPs as HPLC stationary phase for achieving enantioseparation on a preparative scale. Different strategies have been used to overcome this drawback. These include, for instance, the imprinting of relatively inexpensive enantiomers structurally related to the enantiomers of interest. It has been proven that these MIPs generally show some degree of cross-selectivity (or cross-reactivity), property that can be used for the resolution of the (costly) racemic [13–15].

A much less investigated method to achieve enantiomeric separation is the utilization of MIPs prepared with racemic mixtures as templates. In these cases, chirality is introduced into the stationary phase using a chiral functional monomer (or chiral crosslinker). The obvious advantage of this method is that MIP's synthesis requires only the racemate, always available and usually much cheaper than the pure enantiomers. To the best of our knowledge, the first attempt to imprint a racemate was carried-out by Andersson et al. [16] using a chiral crosslinking agent for MIP preparation. The enantioselectivity factor (α) was estimated from batch rebinding experiments and proved to be poor (~1.01). Few years later, Hosoya et al. [4,17] published the first successful examples of imprinting/separation of racemic mixtures using either chiral functional monomer or chiral crosslinker. In one of these articles [17], the synthesis of the new chiral vinyl monomer: (S)-(−)-N-methacryloyl-1-naphthylethylamine (S-MNEA), was reported.

* Corresponding author. Tel.: +54 358 4676523; fax: +54 358 4676233.
E-mail address: cchesta@exa.unrc.edu.ar (C.A. Chesta).

0021-9673/$ – see front matter © 2012 Elsevier B.V. All rights reserved.
http://dx.doi.org/10.1016/j.chroma.2012.09.042

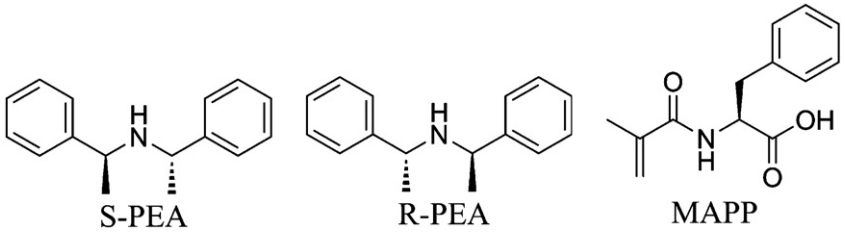

Fig. 1. Chiral templates and chiral functional monomer.

S-MNEA was used to imprint the enantiomers and racemic of N-(3,5-dinitrobenzoyl)-α-methylbenzylamine (R,S-DNB) by the two-step swelling polymerization technique. The reported α were 2.74, 1.69 and 1.40 for S-DNB (MIP-S), R-DNB (MIP-R) and racemic (MIP-RS) imprinted polymers, respectively. Although the mechanism by which Hosoya's polymers were capable of chiral recognition was not investigated in detail, the authors suggested that the enantiomeric discrimination shown by MIP-RS is due to relatively favorable interactions between S-DNB and the recognition sites in the MIP after rebinding.

The main objective of this study is to test Hosoya's approach to the separation of racemic mixtures on methacrylic acid-based MIPs (HPLC) stationary phases using the bulk polymerization technique for MIP preparation. We report herein a study on the enantioseparation of racemic bis[1-phenylethyl]amine (PEA, Fig. 1) on a series of MIPs prepared using the chiral functional monomer (S)-2-(2-methyl-acryloylamino)-3-phenyl propionic acid (MAPP). S- and R-PEA are commercially available chiral auxiliaries, commonly used in the syntheses of β-amino acid esters [18] and optically active butyrolactones [19]. This amine was chosen as target molecule since in a previous study, Spivak et al. [20] showed that racemic PEA can be resolved on chiral methacrylic acid-based MIPs synthesized by the conventional impression technique (i.e., by imprinting just one enantiomers). This background allows the straight comparison between the two imprinting strategies providing a better understanding of the mechanism of enantioseparation in this type of MIPs. MIP-S, MIP-R, MIP-RS (and NIP) were synthesized using PEA enantiomers (and racemic), MAPP, EDGMA as crosslinker and chloroform as porogen. Residence times (t_r), capacity (k') and enantioselectivity (α) factors were estimated from typical elution chromatography experiments. Frontal chromatography experiments were conducted to acquire the adsorption isotherms for both enantiomers on the different MIPs (and NIP). The adsorption isotherms were analyzed using the affinity spectrum (AS) [21–24] and the expectation-maximization (EM) [25,26] methods. This study also involved the theoretical evaluation of the monomer/enantiomers interactions in the pre-polymer mixture. In this aim, standard classical molecular dynamics and docking procedures were applied for obtaining plausible initial structures of R/S-PEA-MAPP complexes, which were later subject of with highly correlated Quantum Mechanics calculations using DFT and an implicit treatment for chloroform as the solvent/porogen. The results obtained from these studies shed some light about the enantiomeric discrimination mechanisms operating in the different MIPs, as we could rely on them for proposing new structures for functional monomers that would enhance the enantioselectivity, on rational bases.

2. Materials and methods

2.1. Reagents

The methacryloyl chloride (97%), ethylene glycol dimethacrylate (EGDMA) (98%), (+)-bis[(R)-1-phenylethyl]amine (R-PEA) (99%) and (−)-bis[(S)-1-phenylethyl]amine (S-PEA) (99%), and chloroform-d ($CDCl_3$) were purchased from Sigma–Aldrich (Argentina). All the solvents were chromatographic grade and used as received. The polymerization initiator, 1,1′-azobis(cyclohexane-1-carbonitrile) (V-40), was provided by Wako Chemicals (USA). EGDMA was purified prior to polymerization using a chromatographic column filled with De-HiBit-200 (Polysciences), which specifically retains the monomer stabilizing agents. The mobile phase modifiers: triethylamine, glacial acetic acid (HAc) and chlorhydric acid were purchased from Merck (Argentina). Triethylamine was distilled prior to use.

2.2. Instrumental

^{1}H NMR spectra were recorded in a Bruker 400 (400 MHz). Mass spectra were recorded on a Bruker, MicroTOF Q II equipment, operated with an ESI source operated in (positive/negative) mode, using nitrogen as nebulizing and drying gas and sodium formate 10 mM as internal calibrant. HPLC chromatographic studies were performed by using a Waters 1525 binary HPLC chromatograph with a manual injector, equipped with a Waters 2487 dual wavelength absorbance detector. Polymerizations were carried-out in a Rayonet photoreactor fitted with four F8T5/BLB Philips UV lamps (λ = 350 nm, 8 W). The MIPs (and NIPs) were grounded manually and sieved to select particles between 25 and 53 μm. Zonytest sieves ASTM 270 (53 μm) and ASTM 500 (25 μm) were used for this purpose. The packing of the analytical columns was done with an Eldex Laboratories pump model AA-100-5-2 eluting at flow rate of 4.5 mL min^{-1}.

2.3. Preparation of (S)-2-(2-methyl-acryloylamino)-3-phenyl propionic acid (MAPP)

MAPP was prepared from (S)-phenylalanine (98%) and methacryloyl chloride following the method published by Lynn et al. [27]. The structure of MAPP was confirmed by mass, ^{13}C and ^{1}H NMR, FT-IR and UV–vis spectroscopy (see SI file).

2.4. Synthesis of MIPs and NIPs

MIP-R, MIP-S, and MIP-RS were synthesized using the bulk polymerization technique from a mixture containing the templates: R-PEA, S-PEA or RS-PEA, respectively, MAPP, EGDMA and V-40 dissolved in chloroform as porogen. The non-imprinted polymers (NIPs) were prepared in the same way but without adding the templates. The polymers were finely grounded in a mortar, dried at 50 °C under reduced pressure (30 Torr) and finally sieved to obtain particles of size between 25 and 53 μm. The polymers were cleaned and packed into the HPLC columns according to the method published elsewhere [28]. Further details of the syntheses, cleaning and packing of the polymers were included as SI. The masses of polymers packed (m_p) into the columns (recovered after the HPLC experiment and dried at 40 °C under reduced pressure for 20 h)

were 0.52, 0.51, 0.60, 0.53 g for MIP-R, MIP-S, MIP-RS, NIP, respectively.

2.5. Elution chromatography and frontal analysis experiments

Columns filled with the different polymers were equilibrated with MeCN/HAc 95:5 (v/v) until a constant UV reference signal was reached. All experiments were performed at an elution rate of 1 mL min^{-1}. The analytes (dead volume marker, R-PEA and S-PEA) were detected by setting the UV detector at 258 nm. All experiments were carried out at room temperature (~300 K). MeCN was used as dead volume marker. The amount injected into the columns was kept constant, i.e. 20 μL of a solution 0.5 mM (10 nmol) of templates. The capacity factors (k') were calculated according to: $k' = (t_r - t_0)/t_0$, where t_r is the analyte retention time and t_0 is the retention time of the unretained solute (MeCN). The selectivity (α) was calculated according to: $\alpha = k'_i/k'_j$, where k'_i and k'_j represent the capacity factor measured either for R- or S-PEA, so that the ratio is always greater than 1.

The experimental data required to construct the adsorption isotherms were obtained from frontal analysis chromatography experiments. The analysis was carried-out following the method published by Sajonz et al. [29], although some few modifications related to the quantification and interpretation of the breakthrough curves, were introduced. Adsorption data was obtained from the desorption breakthrough curves. Eight isotherms were acquired, four corresponding to the desorption of R-PEA on MIP-R, MIP-S, MIP-RS and NIP, and four using S-PEA as the adsorbate.

2.6. Analysis of the adsorption isotherms

The simplest expressions that relate the amount of analyte adsorbed in the stationary phase, $B(C)$ (μmol g^{-1} of polymer), and its concentration at equilibrium in the mobile phase, C (mM), are given by the Langmuir and bi-Langmuir isotherms [30]. However, as shown in Sections 3.1 and 3.2, the Langmuir's isotherm models cannot be used to explain the observed shape and concentration dependence of the chromatographic profiles. Therefore, adsorption isotherms were analyzed using the Freundlich (Eq. (1)) [30] and the general heterogeneous absorption isotherm models (Eq. (2)) [30,31].

The Freundlich isotherm is given by:

$$B(C) = aC^m \tag{1}$$

where m is the heterogeneity factor. m varies from 0 to 1 and decreases as heterogeneity of binding sites increases. The pre-exponential factor a can be associated to the binding affinity of the polymer. The values of a and m obtained from the fitting of the adsorption isotherms to the Freundlich model were used to calculate the distribution of affinity binding sites, $f(K)$ (μmol g^{-1} of polymer), total number of binding sites (f_t, in μmol g^{-1}) and the average affinity of the polymer's binding sites ($\bar{K}$) according to the affinity spectrum method (AS). [21–24] Details of how properties of the polymers are calculated are provided as SI.

The expression of the general heterogeneous absorption isotherm models is given by [31]:

$$B(C) = \int_{-\infty}^{\infty} f(K)\frac{KC}{1+KC}\, d(\ln K) \tag{2}$$

which allows the estimation of $f(K)$ by solving Eq. (2) iteratively within the approximation of the expectation-maximization (EM) [25,26] method. The main advantage of the EM method is that it allows the calculation of $f(K)$ from the raw experimental adsorption isotherm $B(C)$ without assuming explicit models for $f(K)$ or $B(C)$. As indicated above, Eq. (2) is solved iteratively. The algorithm is robust and converges with high stability [31,32]. However, an aspect that remains unclear in the implementation of EM method is how to establish realistic convergence criteria for the iterative procedure. As well pointed-out by Stanley et al. [33] from the statistical point of view, the iteration should continue until the root mean square (rms) error between $B(C)_{cal}$ and $B(C)_{exp}$ is equal to the characteristic noise (or error) of the experimental data. In practice, this error is unknown. Thus, in successive publications, Stanley et al. [33–35] and Guiochon et al. [25,36,37] have used, somehow arbitrarily, 10^4 or 10^6–10^8 iterations to deconvolute Eq. (2). In this article, we adopted a convergence criterion based on the reproducibility of the experimental $B(C)_{exp}$ (see SI).

The parameters obtained from the fitting of the experimental isotherms to Eqs. (1) and (2) were also used to calculate residence times (t_r) applying the ideal chromatography (IC) model. This model, developed by Golshan-Shirazi and Guiochon, assumes infinite column efficiency and mass transfer coefficients that are independent of the concentration of the analyte. Certainly, these assumptions are crude approximations so that the t_r calculated should be regarded as simple estimates [30,38–40]. Details of these calculations are provided as SI. As shown in Section 3.2, the theoretically estimated t_r are used to compare (and validate) the different adsorption isotherms models.

2.7. Molecular modeling

A conformational study was first performed on the separated compounds S-PEA and MAPP. The protocol was as follows: (1) optimization with the AMBER force field [41]. (2) Molecular dynamics: 0.5 ps heating up to 1000 K in the NVE ensemble, with an effective dielectric constant of 10 for simulating chloroform. (3) 500 ps of constant temperature simulation, capturing a maximum of 50 snapshots in the last 250 ps (once every 5 ps). The simulation was run using Gabedit 2.4 [42]. (4) Optimization of the snapshots, picking those within 5 kcal mol^{-1} above the lowest energy minimum. (5) The structures were re-optimized with the hybrid functional B3LYP [43–45] and 6-31G* bases, using the IEFPCM solvent model [46–51].

The lowest energy structures in each case were picked-up for further molecular docking simulations.

From the conformational study was concluded that MAPP was much more flexible than the PEA amines (the latter had the second lowest energy local minimum lying at 7 kcal mol^{-1} above the global minimum; on the other hand, only a few different structures with low energies were found). Thus, the most stable conformers of R- and S-PEA were treated as receptors (and then considered initially fixed) and MAPP was chosen as the flexible ligand in the docking protocol.

The docking procedure was applied using the Autodock 4.2.3 package; further details are available as SI.

The goal of these simulations was just to obtain a set of plausible initial structures for first principles Quantum calculations, by considering all possible favorable interactions between the compounds. This was achieved by the genetic algorithm by trying all possible positions, orientations and torsions, thus avoiding any assumption about the initial structures of the complexes to be calculated by the Quantum approach. The structures selected from the docking simulations were optimized at the B3LYP/6-31G* level of theory, with full geometry optimization in chloroform. Afterwards, both very similar resulting geometries and structures having energies 5 kcal mol^{-1} above of the best in each case were discarded. The energy of the final set of structures of the complexes informed in Table 4 were obtained at the B3LYP/6-311+G(d, p) in IEFPCM [46–51] model for chloroform, together with the energies of the separated compounds in both their neutral and ionic forms. All relative energies informed in Table 4 were taken as the

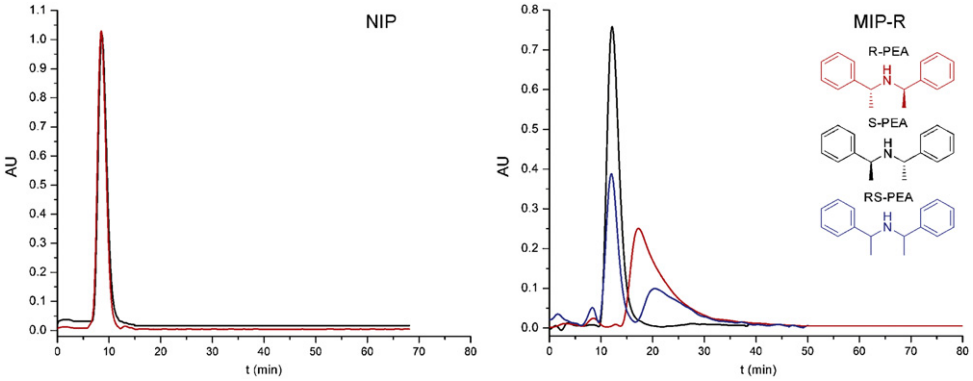

Fig. 2. Elution profiles showing the chiral separation ability of NIP (left) and MIP-R (right): ▬, R-PEA; ─, S-PEA; ▬, R,S-PEA. The sample in all cases is 10 nmol. MeCN/HAc 95:5 (v/v), mobile phase. Flow rate: 1.0 mL min^{-1}. Detection: 258 nm.

differences of the total energies of the complexes and the sum of the total energies of the neutral components R-PEA, S-PEA and MAPP. The species were characterized as minimum by their harmonic frequencies calculations in chloroform; however, since the complexes contain the same type of covalent bonds, no zero point energy corrections were included for computing the relative energies.

All Quantum calculations were carried out with the Gaussian 09 package [52]. The programs Gabedit 2.42 [42] and Molden 4.7 [53] were used for model building and visualization of the results. Molecular graphics were rendered using VMD 1.8.9 [54].

3. Results and discussion

3.1. Study on the selectivity of MIPs by elution chromatography

It has been shown that compounds containing free amino groups can be successfully imprinted and retained in acrylic acid-based MIPs HPLC stationary phases due to strong ion-pair formation interactions [8,10]. To compensate for these strong interactions (and allow for the elution of the analyte), polar mobile phases with high contents of modifiers such as MeCN/HAc, MeCN/amines, and MeCN/HAc/amine (buffers), are usually required [10].

Preliminary elution chromatography experiments intended to investigate the potential of the MIPs synthesized for enantiomeric separation were conducted on MIP-R. The mobile phase chosen for this study was a mixture of MeCN/HAc. As expected, in the absence of the modifier (HAc) the elution of the amine templates does not occur. Thus, a series of experiments varying the composition of the mobile phase from 0.5 to 10% HAc were carried out. From these experiments, it was concluded that concentrations of HAc ~ 4–5% were optimal for the studies, since the chromatograms obtained in such conditions showed acceptable residence times (t_r), peak shapes and enantioselectivity. At concentrations of HAc < 2%, the t_r increased significantly, along with an important broadening of chromatographic profiles. In the presence of 10% HAc almost complete loss of MIP's capacities for enantiomeric separation was observed. The effect of the concentration of HAc on t_r is explained considering that the modifier can interact with both the (acidic) MIPs and the basic amines. HAc can form H-bond with the —COOH groups on the polymers, blocking in part the recognition sites on the surface of the polymer. The acid can also protonate the amine in the mobile phase decreasing the activity of its free form. Both processes cooperate in reducing the binding of the analyte and shortening the residence times [10].

Figs. 2 and 3 show the elution profiles for R-PEA, S-PEA and R, S-PEA on the series of polymers studied. In all injections, and within the experimental uncertainties, t_0 was ~1.9 min. The experimental t_r, capacity (k') and selectivity (α) factors calculated from the chromatograms of the enantiomers injected separately (red and black traces, respectively) are collected in Table 1. It must be here emphasized that the experimental values of t_r (k' and α) have a complex dependence on the amount of analyte injected (n), the mass of polymer packed (m_p) into the columns and obviously, on the nature of the adsorption process (i.e. the adsorption isotherm). Thus, the t_r (k' and α) measured for two different MIPs can be compared only if: (a) the amount of analyte injected is kept constant throughout all experiments [8,55] and (b) the mass of the polymers packed into the columns is the same. In such case, the experimental t_r can be directly related to magnitude of the analyte/polymer interactions. However, the second condition is usually difficult to satisfy. As showed in Section 2.4, and besides the fact the MIPs studied appear morphologically similar, the masses of polymer packed in the column differed. Taken this into consideration,

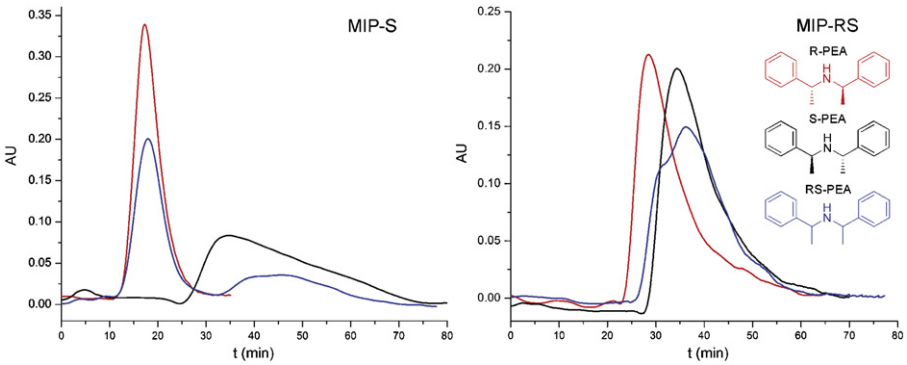

Fig. 3. Elution profiles showing the chiral separation ability of MIP-S (left) and MIP-RS (right): ▬, R-PEA; ─, S-PEA; ▬, R,S-PEA. The sample in all cases is 10 nmol. MeCN/HAc 95:5 (v/v), mobile phase. Flow rate: 1.0 mL min^{-1}. Detection: 258 nm.

Table 1
Retention times (t_r), capacity (k') and selectivity (α) factors calculated from the chromatograms of R-PEA and S-PEA injected separately (sample size 10 nmol).

Polymer	Analyte injected	t_0 (min)	t_r (min)	k'	α	t_r (min)[a]	t_r (min)[b]
NIP	R	1.9	8.4	3.4	1.0	17.9	9.9
	S		8.5	3.5		29.9	9.1
MIP-R	R	1.9	17.3	8.1	1.5	137.0	21.7
	S		12.1	5.4		61.1	17.8
MIP-S	R	1.9	17.2	8.1	2.2	60.3	22.1
	S		34.8	17.3		289.4	36.3
MIP-RS	R	1.9	28.4	13.9	1.2	101.1	26.0
	S		34.4	17.1		157.0	34.1

[a] Values correspond to the approximated retention times calculated using the ideal model of chromatography (IC) for the case of the Freundlich isotherm model (Eq. (13)).
[b] For the case of the Langmuir (Eq. (11)) and bi-Langmuir isotherm (Eq. (12)) models using the parameters estimated by the EM method.

only a qualitative analysis of the elution experiments is possible.

As shown in Fig. 2 (left panel), the NIP is unable to resolve the racemic mixture ($\alpha \sim 1$). In contrast, MIP-R separates the enantiomeric pair showing selectivity for its template (Fig. 2, right panel). The shape of the elution profile (sharp fronting, broadening and the tailing) observed for R-PEA is likely to be caused by a significant heterogeneity of affinity binding sites in the stationary phase [38,56]. In contrast, the less adsorbed isomer S-PEA shows a quasi-Gaussian peak shape. Note that the moles of R- and S-PEA injected to study the racemate (blue traces, Figs. 2 and 3) correspond to half the injected when the enantiomers were studied separately. This dilution effect increases the retention time (t_r) of the enantiomer that interacts more strongly with the MIP (in this case, R-PEA). This behavior is also characteristic of stationary phases showing large binding site's heterogeneity for the template [3,8,38,55]. In Fig. 3 (left panel), the results obtained for MIP-S are shown. As expected, the inversion of the recognition phenomenon is observed. Interestingly, MIP-S shows the largest enantioselectivity factor among the MIPs studied ($\alpha = 2.2$). The dilution effect is also observed and it manifests as an important increase of the t_r observed for S-PEA. Fig. 3 (right panel) shows that MIP-RS is also able to discriminate the enantiomers showing selectivity toward S-PEA ($\alpha = 1.2$). In principle, both enantiomers seem to be affected by dilution and α remains nearly unchanged.

In summary, the MIPs investigated are capable of racemic resolution. However, this capacity varies according to: $\alpha_{MIP\text{-}S} > \alpha_{MIP\text{-}R} > \alpha_{MIP\text{-}RS}$. Interestingly, Hosoya et al. [17] observed the same tendency for the separation of racemic-DNB on MIPs prepared using S-MNEA as functional monomer. Clearly, this agreement may be just coincidental. Hosoya et al. tried to justify the reduced capacity of MIP-RS for enantioseparation using a thermodynamic cycle based on a classical adsorption model. However, the shapes of the chromatographic profiles reported for DNB on the different MIPs studied are clear evidences of large heterogeneities of affinity binding sites affecting these polymers. This fact rules out, indeed, any possibility of interpreting the adsorption phenomena using simple adsorption models. The analysis of the capacity for enantioseparation of the MIPs studied herein is taken up in Section 3.4.

3.2. Analysis of the adsorption isotherms

Frontal chromatography experiments were conducted to acquire adsorption–desorption isotherms for S and R-PEA on the different MIPs (and NIPs). Details of these experiments are given in Section 2.6. In Fig. 4, the adsorption isotherms obtained for S- and R-PEA on MIP-S are compared. In Fig. 4(a) shows the best fits of the adsorption isotherms to the Freundlich model. The fits are poor in both cases ($R^2 < 0.987$). The isotherms show some tendency to saturation at high concentrations that cannot be adequately reproduced by the model. The parameters a and m obtained for all the systems studied are listed in Table 2. These a and m were used to calculate $f(K)$, the number of binding sites (f_t) and the weighted average affinity ($\bar{K}$) according to Eqs. 6–8-SI.

As shown in Table 2, all polymers studied show significant degrees of heterogeneity of binding affinity sites ($m < 1$) and as expected, the heterogeneity is always larger for the most retained (interacting) enantiomer [3,55,57]. The calculated $\bar{K}$ are very similar for all polymers, including the NIP. The polymers differ, however, in the number of specific binding sites. The $f(K)$

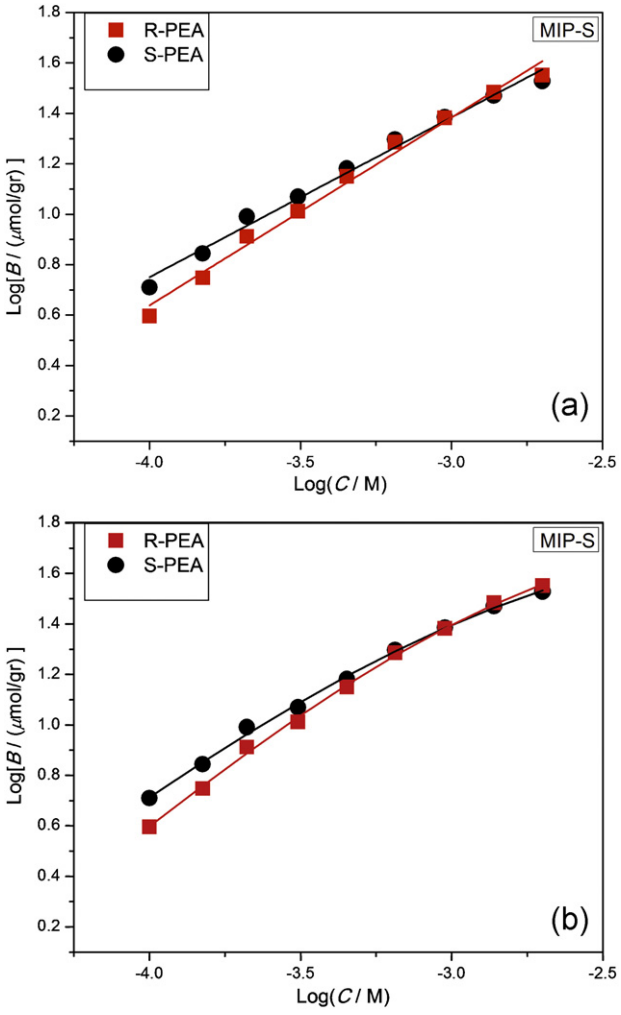

Fig. 4. Experimental binding isotherms for S- and R-PEA on MIP-S. MeCN/HAc 95:5 (v/v), mobile phase. Continuous lines represent the best fits to the Freundlich (a) and to the general heterogeneous absorption isotherm models (b).

Table 2
Experimental a, m, weighted average affinity ($\bar{K}$) and number of binding sites (f_t) calculated for the series of MIPs studied by the AS method. Calculations are for the range $K_{min} = 500\,M^{-1}$ and $K_{max} = 10{,}000\,M^{-1}$.

Polymer	Analyte	a ($\mu mol\,g^{-1}\,M^{-m}$)	m	f_t ($\mu mol\,g^{-1}$)	$\bar{K}$ (M−1)
NIP	R-PEA	2500	0.79	14	1800
	S-PEA	1700	0.73	17	1800
MIP-R	R-PEA	2500	0.68	40	1900
	S-PEA	3000	0.73	31	1900
MIP-S	R-PEA	4200	0.75	37	1800
	S-PEA	1900	0.63	44	2000
MIP-RS	R-PEA	3900	0.73	38	1900
	S-PEA	3400	0.70	44	1900

calculated for S and R-PEA on MIP-S are shown in Fig. 5 (dashed lines). The $f(K)$ for the other polymers are given as SI. As it could be anticipated, both distributions are exponentially decaying functions. As shown in Fig. 5, $f(K)$ is always larger for the isomer-S than for the R, at least in the range of concentration studied. Thus, at low loads of S- or R-PEA (as in the elution experiments) both enantiomers should be able to interact with the binding sites of higher energy (larger K) available. Since the number of recognition sites is larger for S-PEA than for R-PEA (at all K), S-PEA is selectively retained. This explains both, the enantiomer's elution orders (enantioselectivity) and the concentration effect observed on the S-PEA chromatographic profile (Fig. 4, left panel). A similar analysis accounts for the enantioselectivity shown for the other polymers studied. Note that MIP-R and MIP-S show the larger $f(K)$ for their corresponding templates. MIP-RS shows the larger value of $f(K)$ for S-PEA. Table 1 collects the values of t_r calculated from the experimental a and m (Eq. 19-SI). Clearly, the IC model fails to predict the absolute values of the residence times. It gives, however, the correct enantiomer's elution orders (enantioselectivity). It is worth noting that the IC model is extremely sensitive to the value of m. As shown in Table 1-SI, the experimental m are affected by uncertainties of approximately ±5%. This small errors can produce, however, changes in the estimated t_r over ±100 min. Shimizu et al. [22,23,58,59,24] have shown that the values of m obtained by linear regression (with $R^2 > 0.95$) for a series of MIPs are useful for comparing the heterogeneity of the polymers and predicting relative elution orders. However, it seems evident that the values of m calculated from poorly fitted isotherms ($R^2 \sim 0.95$) are not suitable for estimating absolute residence times, at least within the IC model.

The experimental isotherms were also analyzed using the expectation-maximization method (EM) [25,26]. Details of the implementation of the EM method are given Section 2.6. Fig. 4(b) shows the adsorption isotherm for the enantiomers S- and R-PEA on MIP-S fitted to Fredholm's integral (Eq. 16-SI). As shown, the fittings are significantly better than those obtained with the Freundlich model. The results obtained for the other polymers studied are included as SI. The calculated $f(K)$ for S and R-PEA on MIP-S are also plotted in Fig. 6. As expected, the $f(K)$ predicted by the EM and AS methods differ. As shown, an unimodal (Gaussian-like) distribution is obtained for R-PEA, while for S-PEA $f(K)$ the distribution is bimodal. Similar results have been reported by Guiochon and Stanley [26] in the analysis of the adsorption isotherms of a series of enantiomeric pairs on MIPs stationary phases. These authors have referred to the binding sites characterized by large and small $\bar{K}$ as sites of high and low energies, respectively. The values of (f_t) and $\bar{K}$ were calculated by integration of $f(K)$ and $K\,f(K)$ in the $Ln(K)$ space, respectively. In the cases of bimodal distributions, the f_t and $\bar{K}$ were calculated separately. The values of f_t and $\bar{K}$ for all systems studied are collected in Table 3. The corresponding $f(K)$ are included as SI.

As shown in Table 3, all distributions are unimodal except for those obtained for S-PEA on MIP-S and MIP-RS. According to EM method, the NIP shows small population of low affinity sites ($\bar{K} \sim 400\,M^{-1}$). For MIPs, the values of the total number of binding sites ($f_{t1} + f_{t2}$) are larger than those in the NIPs and similar for all polymers. However, the estimated $\bar{K}$ differ. The capability of MIP-R for enantioseparation can be attributed to the larger value of $\bar{K}$ observed for its template or more precisely, to the fact that $f(K)$ is shifted to larger values of K. R-PEA shows similar $\bar{K}_1$ and f_{t1} on MIP-S and MIP-RS, thus the capability of these MIPs for enantiomeric separation can be related to the existence of highly specific binding sites for S-PEA in these polymers (sites 2, Table 3). Although few in number, these highly specific sites are characterized by large $\bar{K}$ ($\sim 10{,}000\,M^{-1}$). Interestingly, when replacing the values of f_t and $\bar{K}$ (Table 3) in the expressions of the Langmuir and bi-Langmuir isotherm models (Eqs. 2-SI and 3-SI), the experimental isotherms are acceptably reproduced (see, Fig. 5-SI). This correlation is due to the relatively narrow distributions calculated by the EM method. In Table 1, the experimental t_r and the corresponding values calculated using the estimated $\bar{K}$ and f_t (and Eqs. 17-SI and 18-SI) are compared. As shown, the IC model slightly overestimates the residence times, but the correlation between the calculated and experimental t_r is quite acceptable (see Fig. 10-SI). Note that the enantiomer's elution orders on the different MIPs are correctly predicted. These results seem to validate the $f(K)$ obtained by the EM method. However, and as expected, the t_r's calculated by the IC model do not predict the large concentration dependence observed in the elution experiments. It is worth to note that the $\bar{K}$ used for the estimation of t_r represents the average of the affinity binding site's distributions. Thus, a better estimation of the residence times (as well as, of its dependence on the amount of analyte injected) could be obtained by solving, within the IC model, the expression of t_r for a continuous distribution $f(K)$. To the best of our knowledge, such a solution has not been reported yet.

Table 3
Experimental average affinity ($\bar{K}$) and total number of binding sites (f_t) calculated for the series of polymers studied using the EM method.

Polymer	Analyte	f_t ($\mu mol\,g^{-1}$)		$\bar{K}$ (M−1)	
		Site 1	Site 2	Site 1	Site 2
NIP	R	36.4	–	430	–
	S	39.4	–	360	–
MIP-R	R	51.5	–	770	–
	S	54.0	–	590	–
MIP-S	R	63.5	–	650	–
	S	51.9	3.4	720	9500
MIP-RS	R	67.5	–	630	–
	S	69.9	1.8	580	13,800

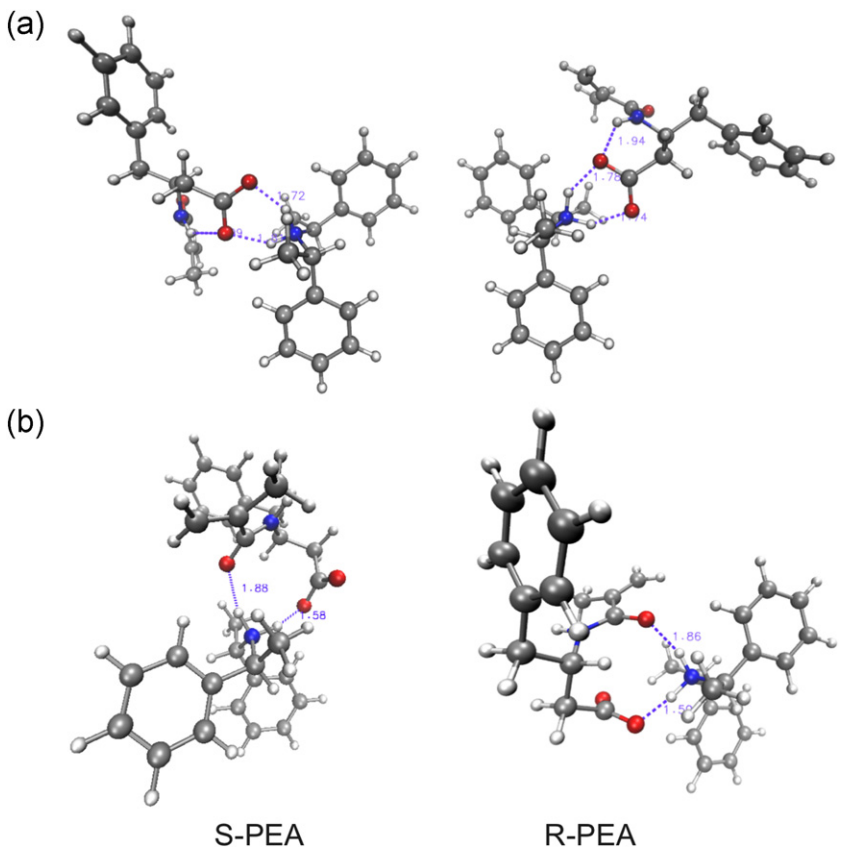

Fig. 5. (a) 3D structures of Complex 1 for S-PEA (left) and R-PEA (right). (b) Complex 3 for S-PEA (left) and Complex 2 for R-PEA (right).

Summarizing, the experimental isotherms were analyzed using the AS and EM methods. As expected, the calculated $f(K)$ differ. However, the conclusions that can be drawn from the analysis of these distributions are similar. Both methods reasonably explain the elution's order and the enantioselectivity observed. Although we have no conclusive evidence, the good fittings of the experimental adsorption isotherms obtained by using the EM method and the acceptable agreement observed between the experimental and theoretically t_r calculated by the IC model, suggest that the $f(K)$ derived from the EM method described better the adsorption phenomena for the MIPs studies.

3.3. Relative stability of diastereomeric pairs in the pre-polymerization mixtures

It is well known that aliphatic amines and carboxylic acids strongly interact forming ion pairs in low and medium polarity solvents [60]. The association constants for the formation of these ionic pairs in the pre-polymerization mixture have been evaluated by spectroscopic titration (UV–vis, NMR, IR, etc.) [61,62] and computational modeling [63,64]. Whilst some authors have built the complexes on reasonable or intuitive bases [66], some other have developed different protocols for considering all possible

Table 4
Summary of B3LYP/6-311+G(d,p) relative energies and equilibrium population at 300 K for the most relevant complexes found in chloroform.

Label	Species[a]	Relative energy (kcal mol^{-1})	f (% at 300 K)
Neutral separated components	S-PEA + MAPP	0.00	
Ionic separated component	S-PEA$^+$ + MAPP$^-$	24.58	
Complex 1	[S-PEA$^+\cdots$MAPP$^-$]	−6.34	19.0
Complex 2		−6.33	18.7
Complex 3		−5.50	4.50
Complex 4		−5.46	4.30
Complex 5		−4.29	0.60
Complex 6		−2.25	0.020
Complex 7		−2.07	0.014
Complex 1	[R-PEA$^+\cdots$MAPP$^-$]	−6.47	23.7
Complex 2		−6.15	13.7
Complex 3		−5.87	8.50
Complex 4		−5.74	6.80
Complex 5		−1.14	0.003
Complex 6		−0.98	0.002
Best neutral pair complex	[R-PEA$\cdots$MAPP]	1.77	0.00002

[a] MAPP$^-$ refers to the anionic (carboxylate) form of MAPP and PEA$^+$ to the cationic (ammonium) form of PEA.

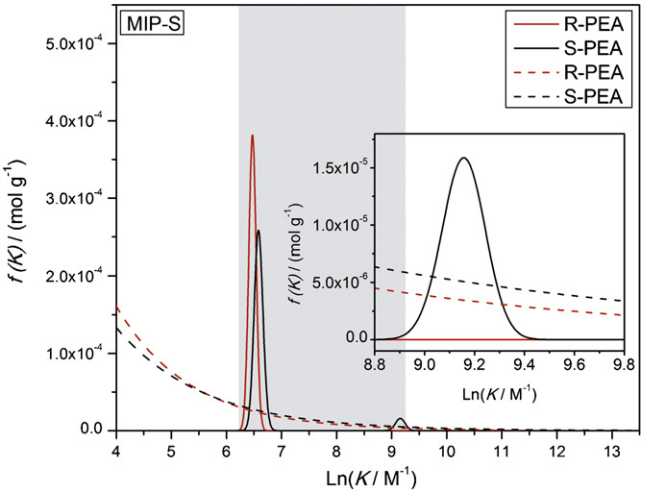

Fig. 6. $f(K)$ for R and S-PEA on MIP-S as calculated by the AS (dashed lines) and EM (solid lines) methods. The highlighted area corresponds to the maximum and minimum concentrations of the enantiomers investigated. Insert: distributions of binding sites for $Ln(K)$ between 8.5 and 10.5.

orientations and torsional degrees of freedom of the molecules which form the pre-polymeric pair [65,66]. In this article we estimate the relative energies of formation of the diastereomeric PEA/MAPP complexes avoiding any assumption about the possible relative orientations or binding modes as described in Section 2.7. Within this procedure, all (or a very large number of) possible complex initial geometries were ranked and the most promising set (in terms of estimated energy) was evaluated by means of first principles QM calculations. The theoretical relative stabilities of the complexes (selected as described in Section 2.7) were calculated and their values summarized on Table 4. These structures should correspond to possible association geometries in chloroform in the pre-polymerization mixture.

As it may be concluded from these energies, MAPP showed no clear preference to form complexes with either the R-PEA or the S-PEA. The Boltzmann factors obtained at 300 K reveal that in a racemic mixture of PEA, the sum of all fractions corresponding to the R-PEA-MAPP and S-PEA-MAPP complexes are 52 and 48%, respectively. The structures of the most stable species formed with each enantiomer are shown on Fig. 5(a).

These poses are characterized by a strong salt bridge between the ammonium and carboxylate groups, with the hydrophobic moieties with slight contact among them but plenty exposed to the chloroform. MAPP is flexible enough for achieving this strong contact, without remarkable torsional strain, irrespectively of the chirality of the ammonium species. Similar features were found for another couple of still important structures for each enantiomer (Complex 2 and 3 of Table 4, with equilibrium populations of about between 4 and 13% at 300 K), shown on Fig. 5(b). In this case also the carbonyl oxygen of MAPP is involved in an H-bond to the ammonium.

Even though both ionic and neutral pairs were considered in the previous modeling and in the subsequent quantum calculations, almost all stable structures included on Table 4 are ionic (i.e. R-PEA or S-PEA as ammonium and MAPP as carboxylate). For comparison purposes, the best neutral pair (one with R-PEA) is included on Table 4, but its energy was fairly higher than those of the ionic pairs (most neutral pairs were discarded before the final refinement with the triple-zeta basis set, since the B3LYP results with the smaller bases showed they were clearly unstable with respect to the ion pairs). The structures and charge distribution of a representative ionic ($R\text{-}PEA^{+}/MAPP^{-}$) and a neutral pair (R-PEA/MAPP) are compared in Fig. 7.

Even though the structure on the right has hydrophobic contacts and one H-bond, it is more than 8 kcal mol^{-1} less stable than the ionic Complex 1 on the left, and also less stable than any of the ionic pair complexes on Table 4. The isosurface corresponds to an electronic density of 0.01 a.u., colored according to the molecular electrostatic potential from −0.10 (red) to +0.14 (blue) at the B3LYP/6-311+G(d,p) level of theory.

According to these computational results, the structure of the complexes should be ionic; this meaning that a proton should be transferred for forming the complex, since the neutral forms are more stable than the ionic ones for the separated components. These calculations also suggest that the energies of formation of diastereomeric pairs $PEA^{+}/MAPP^{-}$ complexes in chloroform should be quite similar.

3.4. The mechanism for enantiodiscrimination

In this section, we analyze in more detail the values of f_t and $\bar{K}$ (Table 3) and its connection with the mechanisms for enantioseparation.

First, it seems necessary to recall that the elution experiments and the adsorption isotherms were acquired using acetonitrile/HAc (5%) as eluent. As commented in Section 3.1, the modifier plays an important role in modulating the PEA/MIPs interactions. Regardless, even in the presence of the modifier, it has been shown that the adsorption of amines on acidic MIPs involves the formation of ion pairs on the surface of polymers [10,61]. It is also interesting to compare the total number of —COOH groups that must be present in the polymers synthesized (∼980 μmol g^{-1}) and the values calculated for f_t (∼40–70 μmol g^{-1}). Clearly, only a reduced number of —COOH groups participate in the recognition processes. This observation agrees with previous studies showing that the acidic modifier can block a large number of recognition sites, particularly those of lower specificity [10,25,36,37].

Comparing the enantiomeric selectivity shown by MIP-R and MIP-S some conclusions about the recognition mechanism can be drawn. During the fabrication of these MIPs, only binding sites for their templates are created. Thus, the fact that both polymers show selectivity for their own templates indicates that the three-dimensional geometries of the recognition sites on MIP-R and MIP-S differ. It can be also concluded that the energy of formation of the ionic-pair complexes between the enantiomers and the —COOH groups attached either to MIP-R or MIP-S surfaces should vary. This fact agrees with the existence of diverse $\bar{K}$ calculated by the EM method for the different enantiomers/MIPs (Table 3). However, this observation contrasts with the theoretical results shown on Section 3.2; i.e., both diastereomeric MAPP/PEA complexes show similar stability in the pre-polymerization mixture. Therefore, the only way to reconcile these observations is to take into account the effect of polymeric matrices. While in the pre-polymerization mixture, the functional monomer and the enantiomers can form ion pair complexes without significant torsional energy costs, the groups surrounding the —COOH in the MIPs should hinder the approach of the adsorbates. Furthermore, the rearrangement of these groups to facilitate the binding process should be prevented by the rigidity of the polymer matrix. This should introduce new (steric) repulsive interactions which end up being the main cause of the observed enantioselectivity. For example, the relative stabilization (per mole of enantiomers) which promotes the specific adsorption of R-PEA on MIP-R can be estimated from the $\bar{K}$ values measure for S- and R-PEA on MIP-R (Table 3) to be ∼−0.2 kcal mol^{-1}. Although small, this difference explains the enantioselectivity shown by MIP-R. Interestingly, this small energy difference makes it difficult to conceive these recognition sites as “specific” binding sites. Apparently, the structures of

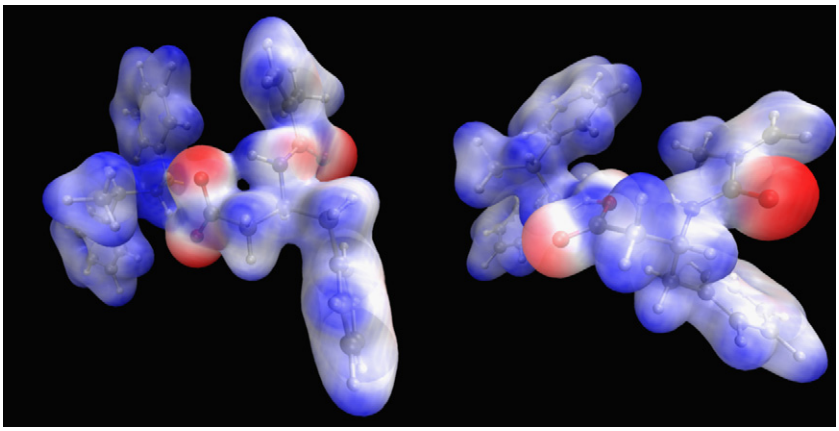

Fig. 7. Best R-PEA$^+$/MAPP$^-$ ionic (left) and neutral R-PEA/MAPP (right) pairs.

these sites are relatively "loosed" and enantioseparation is achieved by small differences in the interaction energy between the enantiomers and the MIP's chiral surface. We are currently performing a series of computational studies with the aim of analyzing the interactions between PEA enantiomers and reduced models of MAPP polymerized with monomers of EDGMA. It is hoped that these studies provide information to confirm or reject this hypothesis.

A similar analysis can be used to explain the enantioselectivity displayed by MIP-S. In this case, the recognition sites of high energy should also be taken into account. However, it is clear that these sites play a minor role in the enantioseparation process. This can be demonstrated by recalculating t_r without considering these sites. The high energy sites added only ~3–4 min to t_r, which are not important for deciding the observed elution order. Unfortunately, the nature/structure of the high energy biding sites cannot be readily elucidated by experimental means. Concerning MIP-RS, it behaves (crudely) as a polymer containing half of binding sites for enantiomer S- and half for R-PEA. Again, the low energy affinity sites seem to control the enantioselectivity shown by this polymer.

Finally, the polymers studied herein are compared to similar MIPs used for the separation of PEA. For instance, Spivak et al. [20], showed that racemic PEA can be separated on a MIP stationary phase prepared by using S-PEA, methacrylic acid as functional monomer, EGDMA as crosslinker agent and methylene chloride as porogen. The enantioselectivity factor (α) estimated from elution experiments for this MIP-S was ~2.2. The eluent used was MeCN/HAc 90:10 (v/v). If this α is compared with the corresponding value on Table 1, it is concluded that Spivak's MIP-R shows a better enantioselectivity. This is evident when considering that the concentration of modifier used by Spivak and col. was twice that used in our study. The reduced ability of MIP-R prepared using MAPP can be explained in terms of the conformational flexibility of MAPP as compared with methacrylic acid. As discussed above, steric forces seem to play a significant role in determining the enantioselectivity of the MIPs. Thus, the magnitude of these forces should increase by forcing the adsorbates to approach the polymer surfaces. If the structures of methacrylic acid and MAPP are compared, it is evident that after polymerization the —COOH groups of methacrylic acid should be located much closer to the polymer surface. Moreover, given its flexibility, MAPP can rearrange to reduce the steric hindrance. Both factors should have negative effects on the enantioseparation process. This suggests that enantioselectivity could be improved optimizing the structure of the functional monomer. At present, we are synthesizing monomers of general structures (Fig. 8).

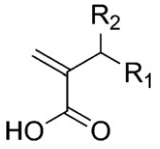

Fig. 8. Chiral functional monomers general structures.

Note that these monomers have the chiral center directly attached to the carbon which is involved in the vinyl polymerization. It is expected that R_1 and R_2 (aromatics or aliphatic groups) will serve to stabilize (or destabilize) preferentially the formation of the diastereomeric ion-pairs complexes (both, in solution and during the rebinding process). The possibility of using chiral crosslinking agents is another option that is being evaluated as a tool for increasing enantiomeric discrimination.

4. Conclusions

In this study we demonstrated that Hosoya's approach to the separation of racemic mixtures on methacrylic acid-based MIPs (HPLC) stationary phases is possible. This is, direct impression of racemic PEA using (S)-2-(2-methyl-acryloylamino)-3-phenyl propionic acid (MAPP) as functional monomer produces a chiral MIP capable to resolve the template.

The adsorption isotherms of PEA enantiomers on MIP-RS, MIP-R and MIP-S were analyzed thoroughly with the aim of obtaining information about the adsorption processes. The experimental isotherms are suitably interpreted by using the general heterogeneous absorption isotherm model (Fredholm's equation). From the analysis of the distributions of recognition sites it is concluded that the MIPs differ in the number and types of affinity binding sites. Interestingly, MIP-R shows unimodal distributions for both enantiomers. The capacity of MIP-R for enantioseparation is attributed to (small) differences in the energies of stabilization of the enantiomers on the surface of the chiral polymer. Taking into account that the theoretical studies indicate that the stabilities of the diastereomeric PEA/MAPP complexes (in solution) should be similar; the observed discrimination might be caused by steric forces that appear only during the enantiomers/polymer rebinding processes. Imprinted polymers fabricated with enantiomer S (MIP-S and MIP-RS) show bimodal distributions of recognition sites of low and high binding energies. However, for both polymers, the capacity for enantiodiscrimination seems to be also given by the low energy biding sites.

These observations depart somehow from the classical view that most researchers have on the structure of MIPs. At least for

the polymers studied herein, results suggest the absence of well structured sites (or cavities) responsible for enantiomeric discrimination. Furthermore, steric hindrance seems to be the main cause of the enantioseparation. Thus, the maximization of these forces may be an important tool for enhancing MIPs capacity.

Acknowledgement

The authors thank the Consejo Nacional de Investigaciones Científicas y Técnicas (CONICET-Argentina), Agencia Nacional de Promoción Científica (FONCYT-Argentina), and Secretaría de Ciencia y Técnica (UNRC) for financial support. J.J.T. and N.G. thanks CONICET-MinCyT (Córdoba) for his PhD scholarship. C.L.R thanks CONICET for her post-doctoral fellowship.

Appendix A. Supplementary data

Supplementary data associated with this article can be found, in the online version, at http://dx.doi.org/10.1016/j.chroma.2012.09.042.

References

[1] M. Yan, O. Ramström, Molecularly Imprinted Materials: Science and Technology, Marcel Dekker, New York, U.S.A., 2005.
[2] Á. Valero-Navarro, M. Gómez-Romero, J.F. Fernández-Sánchez, P.A.G. Cormack, A. Segura-Carretero, A. Fernández-Gutiérrez, J. Chromatogr. A 1218 (2011) 7289.
[3] B. Tóth, K. László, G. Horvai, J. Chromatogr. A 1100 (2005) 60.
[4] K. Hosoya, K. Yoshizako, Y. Shirasu, K. Kimata, T. Araki, N. Tanaka, J. Haginaka, J. Chromatogr. A 728 (1996) 139.
[5] M.C. Moreno-Bondi, F. Navarro-Villoslada, E. Benito-Pena, J.L. Urraca, Curr. Anal. Chem. 4 (2008) 316.
[6] D. Cunliffe, A. Kirby, C. Alexander, Adv. Drug Deliv. Rev. 57 (2005) 1836.
[7] T.A. Sergeyeva, O.A. Slinchenko, L.A. Gorbach, V.F. Matyushov, O.O. Brovko, S.A. Piletsky, L.M. Sergeeva, G.V. Elska, Anal. Chim. Acta 659 (2010) 274.
[8] B. Sellergren, J. Chromatogr. A 906 (2001) 227.
[9] E. Francotte, W. Lindner, Chirality in Drug Research, Wiley-VCH, Weinheim, Germany, 2006.
[10] R.J. Ansell, Adv. Drug Deliv. Rev. 57 (2005) 1809.
[11] M. Kempe, K. Mosbach, J. Chromatogr. A 694 (1995) 3.
[12] N. Maier, W. Lindner, Anal. Bioanal. Chem. 389 (2007) 377.
[13] J. Matsui, K. Fujiwara, T. Takeuchi, Anal. Chem. 72 (2000) 1810.
[14] B.-Y. Huang, Y.-C. Chen, C.-Y. Liu, J. Sep. Sci. 34 (2011) 2293.
[15] H. Wu, Y. Zhao, M. Nie, Z. Jiang, Sep. Purif. Technol. 68 (2009) 97.
[16] L. Andersson, B. Ekberg, K. Mosbach, Tetrahedron Lett. 26 (1985) 3623.
[17] K. Hosoya, Y. Shirasu, K. Kimata, N. Tanaka, Anal. Chem. 70 (1998) 943.
[18] I.T. Barnish, M. Corless, P.J. Dunn, D. Ellis, P.W. Finn, J.D. Hardstone, K. James, Tetrahedron Lett. 34 (1993) 1323.
[19] T. Honda, N. Kimura, M. Tsubuki, Tetrahedron: Asymmetry 4 (1993) 1475.
[20] D.A. Spivak, J. Campbell, Analyst 126 (2001) 793.
[21] D.L. Hunston, Anal. Biochem. 63 (1975) 99.
[22] R.J. Umpleby, S.C. Baxter, Y. Chen, R.N. Shah, K.D. Shimizu, Anal. Chem. 73 (2001) 4584.
[23] R.J. Umpleby, M. Bode, K.D. Shimizu, Analyst 125 (2000) 1261.
[24] R.J. Umpleby, S.C. Baxter, A.M. Rampey, G.T. Rushton, Y. Chen, K.D. Shimizu, J. Chromatogr. B 804 (2004) 141.
[25] H. Kim, G. Guiochon, Anal. Chem. 77 (2005) 1708.
[26] B.J. Stanley, P. Szabelski, Y.B. Chen, B. Sellergren, G. Guiochon, Langmuir 19 (2003) 772.
[27] J. Lynn, J. Org. Chem. 24 (1959) 1030.
[28] J.J. Torres, H.A. Montejano, C.A. Chesta, Macromol. Mater. Eng. 297 (2012) 342.
[29] P. Sajonz, M. Kele, G. Zhong, B. Sellergren, G. Guiochon, J. Chromatogr. A 810 (1998) 1.
[30] G. Guiochon, D.G. Shirazi, A. Felinger, A.M. Katti, Fundamentals of Preparative and Nonlinear Chromatography, Academic Press, San Diego, U.S.A., 1994.
[31] M. Jaroniec, Adv. Colloid Interface Sci. 18 (1983) 149.
[32] P. Szabelski, K. Kaczmarski, A. Cavazzini, Y.B. Chen, B. Sellergren, G. Guiochon, J. Chromatogr. A 964 (2002) 99.
[33] B.J. Stanley, J. Krance, J. Chromatogr. A 1011 (2003) 11.
[34] G. Götmar, B.J. Stanley, T. Fornstedt, G. Guiochon, Langmuir 19 (2003) 6950.
[35] G. Götmar, D. Zhou, B.J. Stanley, G. Guiochon, Anal. Chem. 76 (2003) 197.
[36] H. Kim, G. Guiochon, Anal. Chem. 77 (2005) 1718.
[37] H. Kim, G. Guiochon, Anal. Chem. 77 (2005) 2496.
[38] S. Golshan-Shirazi, G. Guiochon, J. Phys. Chem. 94 (1990) 495.
[39] S. Golshan-Shirazi, G. Guiochon, Anal. Chem. 61 (1989) 462.
[40] H. Kim, K. Kaczmarski, G. Guiochon, Chem. Eng. Sci. 60 (2005) 5425.
[41] W.D. Cornell, P. Cieplak, C.I. Bayly, I.R. Gould, K.M. Merz, D.M. Ferguson, D.C. Spellmeyer, T. Fox, J.W. Caldwell, P.A. Kollman, J. Am. Chem. Soc. 117 (1995) 5179.
[42] A.-R. Allouche, J. Comput. Chem. 32 (2011) 174.
[43] A.D. Becke, Phys. Rev. A 38 (1988) 3098.
[44] C. Lee, W. Yang, R.G. Parr, Phys. Rev. B 37 (1988) 785.
[45] B. Miehlich, A. Savin, H. Stoll, H. Preuss, Chem. Phys. Lett. 157 (1989) 200.
[46] E. Cances, B. Mennucci, J. Chem. Phys. 114 (2001) 4744.
[47] E. Cances, B. Mennucci, J. Tomasi, J. Chem. Phys. 107 (1997) 3032.
[48] D.M. Chipman, J. Chem. Phys. 112 (2000) 5558.
[49] B. Mennucci, E. Cancès, J. Tomasi, J. Phys. Chem. B 101 (1997) 10506.
[50] B. Mennucci, J. Tomasi, J. Chem. Phys. 106 (1997) 5151.
[51] J. Tomasi, B. Mennucci, E. Cancès, J. Mol. Struct.: Theochem. 464 (1999) 211.
[52] M.J. Frisch, G.W. Trucks, H.B. Schlegel, G.E. Scuseria, M.A. Robb, J.R. Cheeseman, G. Scalmani, V. Barone, B. Mennucci, G.A. Petersson, H. Nakatsuji, M. Caricato, X. Li, H.P. Hratchian, A.F. Izmaylov, J. Bloino, G. Zheng, J.L. Sonnenberg, M. Hada, M. Ehara, K. Toyota, R. Fukuda, J. Hasegawa, M. Ishida, T. Nakajima, Y. Honda, O. Kitao, H. Nakai, T. Vreven, J.A. Montgomery Jr., J.E. Peralta, F. Ogliaro, M. Bearpark, J.J. Heyd, E. Brothers, K.N. Kudin, V.N. Staroverov, R. Kobayashi, J. Normand, K. Raghavachari, A. Rendell, J.C. Burant, S.S. Iyengar, J. Tomasi, M. Cossi, N. Rega, J.M. Millam, M. Klene, J.E. Knox, J.B. Cross, V. Bakken, C. Adamo, J. Jaramillo, R. Gomperts, R.E. Stratmann, O. Yazyev, A.J. Austin, R. Cammi, C. Pomelli, J.W. Ochterski, R.L. Martin, K. Morokuma, V.G. Zakrzewski, G.A. Voth, P. Salvador, J.J. Dannenberg, S. Dapprich, A.D. Daniels, O. Farkas, J.B. Foresman, J.V. Ortiz, J. Cioslowski, D.J. Fox, Gaussian 09, Revision A1, Gaussian, Inc., Wallingford, CT, 2009.
[53] G. Schaftenaar, J.H. Noordik, J. Comput. Aided Mol. Des. 14 (2000) 123.
[54] W. Humphrey, A. Dalke, K. Schulten, J. Mol. Graph. 14 (1996) 33.
[55] B. Tóth, T. Pap, V. Horvath, G. Horvai, J. Chromatogr. A 1119 (2006) 29.
[56] G. Guiochon, D.G. Shirazi, A. Felinger, A.M. Katti, Fundamentals of Preparative and Nonlinear Chromatography, Academic Press, San Diego, U.S.A., 2006.
[57] W.-C. Lee, C.-H. Cheng, H.-H. Pan, T.-H. Chung, C.-C. Hwang, Anal. Bioanal. Chem. 390 (2008) 1101.
[58] A.M. Rampey, R.J. Umpleby, G.T. Rushton, J.C. Iseman, R.N. Shah, K.D. Shimizu, Anal. Chem. 76 (2004) 1123.
[59] R.J. Umpleby, S.C. Baxter, M. Bode, J.K. Berch Jr., R.N. Shah, K.D. Shimizu, Anal. Chim. Acta 435 (2001) 35.
[60] D.F. DeTar, R.W. Novak, J. Am. Chem. Soc. 92 (1970) 1361.
[61] R.J. Ansell, K.L. Kuah, Analyst 130 (2005) 179.
[62] J. O'Mahony, A. Molinelli, K. Nolan, M.R. Smyth, B. Mizaikoff, Biosens. Bioelectron. 20 (2005) 1884.
[63] J. Jiang, K. Song, Z. Chen, Q. Zhou, Y. Tang, F. Gu, X. Zuo, Z. Xu, J. Chromatogr. A 1218 (2011) 3763.
[64] B.r.C.G. Karlsson, J. O'Mahony, J.G. Karlsson, H. Bengtsson, L.A. Eriksson, I.A. Nicholls, J. Am. Chem. Soc. 131 (2009) 13297.
[65] H. Zhang, T. Song, F. Zong, T. Chen, C. Pan, Int. J. Mol. Sci. 9 (2008) 98.
[66] L.E. Gómez-Pineda, G.E. Pina-Luis, C.M. Cortés-Romero, M.E. Palomar-Pardavé, G.A. Rosquete-Pina, M.E. Díaz-García, M.d.l.A.C. Hernández, Molecules 15 (2010) 4017.